Design and Flight Performance of the Orion Pre-Launch Navigation System

Renato Zanetti*

NASA Johnson Space Center, Houston, Texas, 77058, USA

Launched in December 2014 atop a Delta IV Heavy from the Kennedy Space Center, the Orion vehicle's Exploration Flight Test-1 (EFT-1) successfully completed the objective to test the prelaunch and entry components of the system. Orion's pre-launch absolute navigation design is presented, together with its EFT-1 performance.

I. Introduction

The Orion capsule, the successor of the Space Shuttle as NASA's flagship human transportation vehicle, is designed to take men back to the Moon and beyond. The first Exploration Mission (EM1) is scheduled for 2018, while its first flight test, EFT-1 (Exploration Flight Test-1), was successfully completed on December 5th, 2014. The main objective of the test was to demonstrate the capability to re-enter the Earth's atmosphere and achieve safe splash-down into the Pacific Ocean. This un-crewed mission completes two orbits around Earth, the second of which was highly elliptical with an apogee of approximately 5908 km, higher than any vehicle designed for humans since the Apollo program. The trajectory was designed in order to test a high-energy re-entry similar to those crews will undergo during lunar missions. In order to have a good navigation solution during entry, the navigation system operated during pre-flight operations, and during the entire flight, even when Orion was not controlling itself but under the control of the launch vehicle or the upper stage.

Reference **?** describes the navigation design of Orion's EFT-1 mission and the flight performance for the post-lift phase. The objectives of this paper are to: i. introduce the pad align algorithm design of the Orion vehicle, both the Exploration Flight Test 1 design and the changes made in preparation for Exploration Missions 1 and 2, and ii. document the performance of the pre-launch navigation system during EFT-1, which relies on the classic extended Kalman filter (EKF).[2] Reference 3 introduced the preliminary EFT-1 navigation design, while pre-mission simulation performance was shown in reference. 4. The UDU factorization as introduced by Bierman is employed in the filter design,[5] and measurements are included as scalars employing the Carlson[6] and Agee-Turner[7] Rank-One updates. The possibility of considering only some of the filter's states (rather than estimating all of them[8]) is included in the design.[9]

Prior to launch the extended Kalman filter is initialized with the estimated vehicle's attitude from gyro compassing (coarse align algorithm) and an inertial position derived from the current time and the coordinates of the pad. This pre-launch navigation phase is called fine align and the only measurement active in this mode during EFT-1 was integrated velocity, which is a pseudo-measurement consisting of a zero change of Earth-referenced position over a 1 second interval. The GPS receiver measurement are not available during fine align because the vehicle, including the GPS antennas, are covered by the launch abort fairing. The main purpose of fine align is to better estimate the attitude and the IMU error states.

II. Inertial Measurement Unit

II.A. The Gyro Model

The gyro is modeled in terms of the bias, scale factor, and non-orthogonality. The IMU *case frame* is defined such that the x-axis of the gyro is the reference direction with the $x-y$ plane being the reference

*GN&C Autonomous Flight Systems Engineer, Aeroscience and Flight Mechanics Division, EG6, 2101 NASA Parkway. AIAA Associate Fellow.

plane; the y- and z-axes are not mounted perfectly orthogonal to it (this is why we don't have a full misalignment/nonorthogonality matrix as we will in the accelerometer model). The errors in determining these misalignments are the so-called *non-orthogonality errors*, expressed as a matrix $\mathbf{\Gamma}$, as

$$\mathbf{\Gamma}^g = \begin{bmatrix} 0 & \gamma_3^g & \gamma_2^g \\ \gamma_3^g & 0 & \gamma_1^g \\ \gamma_2^g & \gamma_1^g & 0 \end{bmatrix}$$

The gyro scale factor represents the error in conversion from raw sensor outputs (gyro digitizer pulses) to useful units. In general we model the scale-factor error as a first-order Markov (or a Gauss-Markov) process in terms of a diagonal matrix given as

$$\mathbf{S}^g = \begin{bmatrix} s_x^g & 0 & 0 \\ 0 & s_y^g & 0 \\ 0 & 0 & s_z^g \end{bmatrix}$$

Similarly, the gyro bias errors are modeled as as first-order vector Gauss-Markov processes as

$$\boldsymbol{b}^g = \begin{bmatrix} b_x^g \\ b_y^g \\ b_z^g \end{bmatrix}$$

Finally, the gyro noise is represented by $\boldsymbol{\epsilon}_g$. Hence the model of the gyro measurement is given by

$$\boldsymbol{\omega}_m^c = \left(\mathbf{I}_3 + \mathbf{\Gamma}^g + \mathbf{\Delta}^g\right)\left(\boldsymbol{\omega}^c + \boldsymbol{b}_g + \boldsymbol{\epsilon}_g\right) = \left(\mathbf{I}_3 + \mathbf{\Delta}^g\right)\left(\boldsymbol{\omega}^c + \boldsymbol{b}_g + \boldsymbol{\epsilon}_g\right) \tag{1}$$

where $\boldsymbol{I}_3$ is a 3×3 identity matrix, the superscript c indicates that this is an inertial measurement at the 'box-level' expressed in *case-frame* co-ordinates, and $\boldsymbol{\omega}^c$ is the 'true' angular velocity in the case frame. Notice that since $(\mathbf{I} + \mathbf{\Delta}^g)^{-1} \approx \mathbf{I} - \mathbf{\Delta}^g$, we can express the actual angular velocity in terms of the measured angular velocity as

$$\boldsymbol{\omega}^c = \left(\mathbf{I}_3 - \mathbf{\Delta}^g\right)\boldsymbol{\omega}_m^c - \boldsymbol{b}_g - \boldsymbol{\epsilon}_g \tag{2}$$

The actual measurement provided by gyros is the the accumulated angle:

$$\left(\Delta\boldsymbol{\theta}_{c_{k-1}}^{c_k}\right)_m = \int_{t_{k-1}}^{t_k} \boldsymbol{\omega}_m^c(\tau) + \frac{1}{2}\boldsymbol{\phi}_{c_{ref}}^c \times \boldsymbol{\omega}_m^c(\tau)\, d\tau \tag{3}$$

$$= \int_{t_{k-1}}^{t_k} \boldsymbol{\omega}_m^c(\tau) + \frac{1}{2}\left[\int_{t_{k-1}}^{\tau} \dot{\boldsymbol{\phi}}_{c_{ref}}^c(\chi)\, d\chi\right] \times \boldsymbol{\omega}_m^c(\tau)\, d\tau \tag{4}$$

$$= \int_{t_{k-1}}^{t_k} \boldsymbol{\omega}_m^c(\tau) + \frac{1}{2}\left[\int_{t_{k-1}}^{\tau} \left(\boldsymbol{\omega}_m^c(\chi) + \frac{1}{2}\boldsymbol{\phi}_{c_{ref}}^c \times \boldsymbol{\omega}_m^c(\chi)\right) d\chi\right] \times \boldsymbol{\omega}_m^c(\tau)\, d\tau$$

Ignoring second-order terms, we get

$$\left(\Delta\boldsymbol{\theta}_{c_{k-1}}^{c_k}\right)_m = \int_{t_{k-1}}^{t_k} \left[\boldsymbol{\omega}_m^c(\tau) + \frac{1}{2}\int_{t_{k-1}}^{\tau} \boldsymbol{\omega}_m^c(\chi)\; d\chi \times \boldsymbol{\omega}_m^c(\tau)\right] d\tau \tag{5}$$

II.B. The Accelerometer Model

Similar to the gyros, the accelerometer scale factor represents the error in conversion from raw sensor outputs (accelerometer digitizer pulses) to useful units. In general we model the scale-factor error as a first-order (Gauss-) Markov process in terms of a diagonal matrix given as

$$\mathbf{S}^a = \begin{bmatrix} s_x^a & 0 & 0 \\ 0 & s_y^a & 0 \\ 0 & 0 & s_z^a \end{bmatrix}$$

Similarly, the bias errors are modeled as as first-order Gauss-Markov processes as

$$\boldsymbol{b}^a = \begin{bmatrix} b_x^a \\ b_y^a \\ b_z^a \end{bmatrix}$$

So, the accelerometer measurements, $\boldsymbol{a}_m^c$ are modeled as:

$$\boldsymbol{a}_m^c = (\boldsymbol{I}_3 + \boldsymbol{S}^a)(\boldsymbol{a}^c + \boldsymbol{b}^a + \boldsymbol{\upsilon}_a) \tag{6}$$

where $\boldsymbol{I}_3$ is a 3×3 identity matrix, the superscript c indicates that this is an inertial measurement at the 'box-level' expressed in *case-frame* co-ordinates, and $\boldsymbol{a}^c$ is the 'true' non-gravitational acceleration in the case frame. The quantity $\boldsymbol{\upsilon}_a$ is the velocity random walk, a zero-mean white sequence on acceleration that integrates into a velocity random walk, which is the 'noise' on the accelerometer output. We note that the measured $\Delta\mathbf{v}$ in the case frame, $\Delta\mathbf{v}_m^c$, is mapped to the end of it's corresponding time interval by the sculling algorithm within the IMU firmware, so that we can write

$$(\Delta\mathbf{v}_m^c)_k = \int_{t_{k-1}}^{t_k} \mathbf{T}_{c(t)}^{c_k} \mathbf{a}_m^{c(t)} dt \tag{7}$$

where $(\Delta\mathbf{v}_m^c)_k$ covers the time interval from t_{k-1} to t_k ($t_k > t_{k-1}$) and $c(t)$ is the instantaneous case frame[a]. We recall that a transformation matrix can be written in terms of the Euler axis/angle as

$$\begin{aligned} T(\boldsymbol{\phi}) &= \cos(\phi)\boldsymbol{I} - \frac{\sin\phi}{\phi}[\boldsymbol{\phi}\times] + \frac{1-\cos\phi}{\phi^2}\boldsymbol{\phi}\boldsymbol{\phi}^T & (10) \\ &= \boldsymbol{I} - \frac{\sin\phi}{\phi}[\boldsymbol{\phi}\times] + \frac{1-\cos\phi}{\phi^2}[\boldsymbol{\phi}\times][\boldsymbol{\phi}\times] & (11) \end{aligned}$$

which, for $\boldsymbol{\phi} \sim \mathbf{0}$ can be approximated as

$$T(\boldsymbol{\phi}) = \boldsymbol{I} - [\boldsymbol{\phi}\times] \tag{12}$$

With this in mind, $\mathbf{T}_{c(t)}^{c_k} = \mathbf{I}_3 - \left[\boldsymbol{\theta}_{c(t)}^{c_k}\times\right]$, and using Eq. (6), $\left(\Delta\mathbf{v}_m^B\right)_k$ becomes

$$(\Delta\mathbf{v}_m^c)_k = \int_{t_{k-1}}^{t_k} \left[\mathbf{I}_3 - \left[\boldsymbol{\theta}_{c(t)}^{c_k}\times\right]\right] \left[(\boldsymbol{I}_3 + \boldsymbol{\Delta}^a)\boldsymbol{a}^c + \boldsymbol{b}^a + \boldsymbol{\upsilon}_a\right] dt \tag{13}$$

We can expand this equation, neglecting terms of second-order, as follows

$$\begin{aligned} (\Delta\mathbf{v}_m^c)_k &= \int_{t_{k-1}}^{t_k} \left[\mathbf{I}_3 - \left[\boldsymbol{\theta}_{c(t)}^{c_k}\times\right]\right] \boldsymbol{a}^c dt + \int_{t_{k-1}}^{t_k} (\boldsymbol{b}^a + \boldsymbol{\upsilon}_a)\, dt \\ &\quad + \int_{t_{k-1}}^{t_k} \boldsymbol{\Delta}^a \boldsymbol{a}^c dt \end{aligned} \tag{14}$$

The first term in the above equation (Eq. (14)) becomes

$$\int_{t_{k-1}}^{t_k} \left[\mathbf{I}_3 - \left[\boldsymbol{\theta}_{c(t)}^{c_k}\times\right]\right] \boldsymbol{a}^c dt = (\Delta\mathbf{v}^c)_k \tag{15}$$

[a]Or equivalently,

$$\left(\Delta\mathbf{v}_m^B\right)_k = \int_{t_{k-1}}^{t_k} \mathbf{T}_{B(t)}^{B_k} \mathbf{a}_m^{B(t)} dt \tag{8}$$

But since $\mathbf{T}_{B(t)}^{B_k} \approx \mathbf{I}_3 - \left[\boldsymbol{\phi}_{B(t)}^{B_k}\times\right]$, we find

$$\left(\Delta\mathbf{v}_m^B\right)_k = \int_{t_{k-1}}^{t_k} \left[\mathbf{I}_3 - \left[\boldsymbol{\phi}_{B(t)}^{B_k}\times\right]\right] \mathbf{a}_m^{B(t)} dt \tag{9}$$

and the third term becomes

$$\int_{t_{k-1}}^{t_k} \boldsymbol{\Delta}^a \boldsymbol{a}^c dt = \boldsymbol{\Delta}^a \int_{t_{k-1}}^{t_k} \boldsymbol{a}^c dt \approx \boldsymbol{\Delta}^a \left(\Delta \mathbf{v}^c\right)_k \tag{16}$$

Finally, the accelerometer noise, which is zero-mean process with spectral density $\mathbf{S}_a$ becomes

$$\int_{t_k}^{t_{k+1}} \boldsymbol{v}_a dt = \mathbf{u}_a \tag{17}$$

where $\mathbf{u}_a$ is a random vector with covariance $\mathbf{S}_a(t_k - t_{k-1})$. So, Eq. (14) becomes

$$\left(\Delta \mathbf{v}_m^c\right)_k = \left[\mathbf{I}_3 + \boldsymbol{\Delta}^a\right] \left(\Delta \mathbf{v}^c\right)_k + \boldsymbol{b}^a \Delta t + \boldsymbol{v}_a \Delta t \tag{18}$$

Since we have established that $\left[\mathbf{I}_3 + \boldsymbol{\Delta}^a\right]^{-1} \approx \left[\mathbf{I}_3 - \boldsymbol{\Delta}^a\right]$, and neglecting terms of second-order,

$$\left(\Delta \mathbf{v}^c\right)_k = \left[\mathbf{I}_3 - \boldsymbol{\Delta}^a\right] \left(\Delta \mathbf{v}_m^c\right)_k - \boldsymbol{b}^a \Delta t - \boldsymbol{v}_a \Delta t \tag{19}$$

III. Coarse Align Design

The Coarse Align Computer Software Unit (CSU) main purpose is to compute an initial guess of the attitude of the Orion vehicle while on the pad. The output attitude is based on a simple filtering of high rate IMU data with the assumption that the vehicle is standing still.

Orion IMU sensor sampling is at 1600 Hz to accommodate high rate compensations such as coning, sculling, size effect and accelerometer digitizer asymmetry compensation. The 1600 Hz data is used to form compensated 200 Hz delta angles and delta velocities in the body frame. The 200 Hz data is organized in buffers and passed to the VMC at a 40 Hz rate to ensure that no sample is lost.

Low pass second order filters are applied to the IMU measurements to remove noise and oscillatory motion due to wind (twist and sway). The expected output of the Coarse Alignment, T_e^b, is the attitude of the vehicle body-fixed frame (b) with respect to the Earth-fixed frame (e, or International Terrestrial Reference Frame, ITRF). An intermediate calculation is T_{ned}^b, that represents the transformation matrix of the vehicle attitude with respect to the North-East-Down (NED) frame.

The NED frame is derived from the filtered body frame vectors as follows:
"Up" is defined as the unit filtered delta-velocity vector in the body frame

$$\hat{\mathbf{U}} = \frac{\Delta \mathbf{v}_{ib}^b}{|\Delta \mathbf{v}_{ib}^b|}$$

"East" is defined as the unit filtered delta-angle (earth rate) vector crossed with "Up"

$$\hat{\mathbf{E}} = \frac{\Delta \boldsymbol{\theta}_{ib}^b \times \hat{\mathbf{U}}}{|\Delta \boldsymbol{\theta}_{ib}^b \times \hat{\mathbf{U}}|}$$

"North" is defined as the cross product of "Up" and "East"

$$\hat{\mathbf{N}} = \frac{\hat{\mathbf{U}} \times \hat{\mathbf{E}}}{|\hat{\mathbf{U}} \times \hat{\mathbf{E}}}$$

$$T_{ned}^b = \begin{bmatrix} \hat{N}_x & \hat{E}_x & -\hat{U}_x \\ \hat{N}_y & \hat{E}_y & -\hat{U}_y \\ \hat{N}_z & \hat{E}_z & -\hat{U}_z \end{bmatrix}$$

$$T_e^b = T_{ned}^b \times T_e^{ned}$$

The transformation matrix T_e^{ned} is determined from the surveyed coordinates of the pad.

Note that a potential singularity exists in this algorithm if the $\Delta \mathbf{v}_{ib}^b$ and $\Delta \boldsymbol{\theta}_{ib}^b$ vectors are co-linear. Although this condition should not occur unless the alignment is done at the north or south pole, a check is made to ensure the $|\Delta \boldsymbol{\theta}_{ib}^b \times \hat{\mathbf{U}}|$ is of reasonable size prior to computing $\hat{\mathbf{E}}$. If this is not the case then T_{ned}^b should be set to the identity transform.

IV. Navigation Algorithm Design

Measurements are incorporated in the navigation solution at 1Hz, which is a typical rate of GPS sensors. However the attitude control algorithm necessitates estimates from the navigation solution at a higher rate, furthermore the IMU measurement data is available at a higher rate. The delta velocity delta attitude accumulator (DVDAAccum) CSU is the high-rate Inertial Measurement Unit (IMU) accumulator and attitude propagator complement to filter CSUs in the 1 Hz rate group. The vehicle attitude is propagated forward in time through the use of accumulated sensed $\Delta\boldsymbol{\theta}$ data. The CSU also accumulates ΔV measurements which are used by the Position and Velocity Fast Propagator to compute high rate position and velocity for downstream users. The attitude of DVDAAccum is re-synched to the 1 Hz rate group estimate each second.

DVDAAccum receives feedback data from the 1 Hz EKF CSUs and uses it to perform an update. During the update phase DVDAAccum replaces the estimates of the IMU errors with the most current values, transforms the values of the inertial accumulated delta velocity into the updated inertial frame, and updates the inertial to Orion body attitude with the information from the filter.

The Orion fine alignment algorithm utilizes the same Extended Kalman Filter architecture and CSU as that used for atmospheric navigation (ATMEKF, used during the fine align, ascent, and entry phases). This paper presents the design of the fine align portion of the algorithm and trades between three different type of fine align measurements: Integrated Velocity (IV), Zero Velocity (ZV), and Pad Position (Pos). All these measurements are pseudomeasurents, no sensor exists that produces them, instead the measurements are derived from the fact that the vehicle is not moving with respect to the pad. Hence the actual measurement utilized from the filter is the theoretical value and the measurement noise is given by the variation from this theoretical value due to twist and sway motion of the stack. This motion is forced by wind and is a function of the bending modes of the launch system.

During EFT-1, the Orion EKF used an IV measurement, to precisely estimate the attitude of the IMU on the launch pad during the fine align phase. For EM1 and beyond, three possible solutions are considered:

1. The IV measurement returns the change in Earth Centered Earth Fixed (ECEF) position over a specified amount of time, typically the call rate of the EKF, which for EFT-1 is one second. This is a "fake" measurement since no sensor exist and the processed measurement is always given by the nominal value of zero. The measurement noise is therefore given by the true motion of the IMU due to twist and sway of the stack.

2. The pad position (Pos) measurement returns the planet-fixed position of the IMU. This is also a "fake" measurement always set to the nominal location. The measurement error is comprised not only to the twist and sway motion, but also of the survey error of the pad location. Therefore the measurement error has two distinct contributors, a varying component due to the stack oscillations and a repeatable component due to the survey errors.

3. The zero velocity (ZV) measurement returns the instantaneous planet-fixed velocity of the IMU. This is also a "fake" measurement always set to the nominal value of zero. The measurement noise is given by the true motion of the IMU due to twist and sway of the stack.

IV.A. Integrated Velocity

Given the current inertial position $\mathbf{r}^i$ at time t, the prior inertial position $\mathbf{r}_0^i$, as well as the transformation matrix between Earth-fixed and inertial ($\mathbf{T}_e^i$), the IV measurement is given by

$$\mathbf{y}_{IV} = \mathbf{h}_{IV}(\mathbf{x}, \mathbf{x}_0, t) = \left(\mathbf{T}_e^i(t)\right)^T \mathbf{r}^i - \left(\mathbf{T}_e^i(t_0)\right)^T \mathbf{r}_0^i + \boldsymbol{\eta}_{IV} = \mathbf{0} \tag{20}$$

where $\mathbf{h}_{IV}(\mathbf{x}, \mathbf{x}_0, t)$ is the measurement model (note the transpose on the transformation matrix) and $\boldsymbol{\eta}_{IV}$ is the measurement noise which exactly cancels out the motion due to twist and sway. The estimated measurement is given by

$$\hat{\mathbf{y}}_{IV} = \mathbf{h}_{IV}(\hat{\mathbf{x}}, \hat{\mathbf{x}}_0, t) = \left(\mathbf{T}_e^i(t)\right)^T \hat{\mathbf{r}}^i - \left(\mathbf{T}_e^i(t_0)\right)^T \hat{\mathbf{r}}_0^i \tag{21}$$

notice that this measurement is nonlinear, potentially highly-nonlinear, since in order to calculate the prior inertial position is necessary to back-integrate the nonlinear equations of motion that also contain the

estimates of the IMU error parameters. Therefore, the measurement residual is

$$\boldsymbol{\epsilon}_{IV} = \mathbf{y}_{IV} - \hat{\mathbf{y}}_{IV} \tag{22}$$

As a first order approximation (used to obtain the IV measurement partials or measurement mapping matrix $\mathbf{H}_{IV}$)

$$\begin{aligned}
\boldsymbol{\epsilon}_{IV} &= \frac{\partial \mathbf{h}_{IV}}{\partial \mathbf{x}}(\mathbf{x} - \hat{\mathbf{x}}) + \frac{\partial \mathbf{h}_{IV}}{\partial \mathbf{x}_0}(\mathbf{x}_0 - \hat{\mathbf{x}}_0) + \boldsymbol{\eta}_{IV} && (23)\\
&= \frac{\partial \mathbf{h}_{IV}}{\partial \mathbf{x}}\hat{\mathbf{x}} + \frac{\partial \mathbf{h}_{IV}}{\partial \mathbf{x}_0}\boldsymbol{\Phi}(t, t_0)\hat{\mathbf{x}} + \boldsymbol{\eta}_{IV} && (24)\\
&= \mathbf{H}_{IV}(\hat{\mathbf{x}})\,(\mathbf{x} - \hat{\mathbf{x}}) + \boldsymbol{\eta}_{IV} && (25)
\end{aligned}$$

where $\boldsymbol{\Phi}(t, t_0)$ is the state transition matrix. With this in mind, the partial derivative of the IV measurement is as follows

$$\begin{aligned}
\frac{\partial \mathbf{h}_{IV}}{\partial \mathbf{r}}(\hat{\mathbf{x}}) &= \left(\mathbf{T}_e^i(t)\right)^T - \left(\mathbf{T}_e^i(t_0)\right)^T \Phi_{\mathbf{rr}}(t, t_0) && (26)\\
\frac{\partial \mathbf{h}_{IV}}{\partial \mathbf{v}}(\hat{\mathbf{x}}) &= -\left(\mathbf{T}_e^i(t_0)\right)^T \Phi_{\mathbf{rv}}(t, t_0) && (27)\\
\frac{\partial \mathbf{h}_{IV}}{\partial \boldsymbol{\phi}}(\hat{\mathbf{x}}) &= -\left(\mathbf{T}_e^i(t_0)\right)^T \Phi_{\mathbf{r}\boldsymbol{\phi}}(t, t_0) && (28)\\
\frac{\partial \mathbf{h}_{IV}}{\partial \mathbf{b}_a}(\hat{\mathbf{x}}) &= -\left(\mathbf{T}_e^i(t_0)\right)^T \Phi_{\mathbf{rb}_a}(t, t_0) && (29)\\
\frac{\partial \mathbf{h}_{IV}}{\partial \mathbf{s}_a}(\hat{\mathbf{x}}) &= -\left(\mathbf{T}_e^i(t_0)\right)^T \Phi_{\mathbf{rs}_a}(t, t_0) && (30)\\
\frac{\partial \mathbf{h}_{IV}}{\partial \boldsymbol{\xi}_a}(\hat{\mathbf{x}}) &= -\left(\mathbf{T}_e^i(t_0)\right)^T \Phi_{\mathbf{r}\boldsymbol{\xi}_a}(t, t_0) && (31)\\
\frac{\partial \mathbf{h}_{IV}}{\partial \mathbf{b}_g}(\hat{\mathbf{x}}) &= -\left(\mathbf{T}_e^i(t_0)\right)^T \Phi_{\mathbf{rb}_g}(t, t_0) && (32)\\
\frac{\partial \mathbf{h}_{IV}}{\partial \mathbf{s}_g}(\hat{\mathbf{x}}) &= -\left(\mathbf{T}_e^i(t_0)\right)^T \Phi_{\mathbf{rs}_g}(t, t_0) && (33)\\
\frac{\partial \mathbf{h}_{IV}}{\partial \boldsymbol{\gamma}_g}(\hat{\mathbf{x}}) &= -\left(\mathbf{T}_e^i(t_0)\right)^T \Phi_{\mathbf{r}\boldsymbol{\gamma}_g}(t, t_0) && (34)
\end{aligned}$$

The measurement noise is given by the change in position due to sway over one second. Notice that because of the back-propagation, this measurement is nonlinear in nature. Due to the oscillatory motion due to the flex modes of the stack, this nonlinearity could be potentially severe, although severe nonlinearities are not expected over one second intervals nor were they experience during EFT-1.

IV.B. Pad Position Measurement

The position measurement is expressed as follows:

$$\mathbf{y}_{Pos} = \mathbf{h}_{Pos}(\mathbf{x}, t) = \left(\mathbf{T}_e^i(t)\right)^T \mathbf{r}^i + \mathbf{b}_{pad} + \boldsymbol{\eta}_{Pos} \tag{35}$$

where $\mathbf{b}_{pad}$ is the launch pad location survey error and $\boldsymbol{\eta}_{Pos}$ is the measurement noise which exactly cancels out the motion due to twist and sway. The estimated measurement is given by

$$\hat{\mathbf{y}}_{Pos} = \mathbf{h}_{Pos}(\hat{\mathbf{x}}, t) = \left(\mathbf{T}_e^i(t)\right)^T \hat{\mathbf{r}}^i + \hat{\mathbf{b}}_{pad} \tag{36}$$

The measurement residual is

$$\boldsymbol{\epsilon}_{Pos} = \mathbf{y}_{Pos} - \hat{\mathbf{y}}_{Pos} = \mathbf{H}_{Pos}(\hat{\mathbf{x}})\,\hat{\mathbf{x}} + \boldsymbol{\eta}_{Pos} \tag{37}$$

With this in mind, the partial derivative of the position measurement is as follows

$$\frac{\partial \mathbf{h}_{Pos}}{\partial \mathbf{r}}(\hat{\mathbf{x}}) = \left(\mathbf{T}_e^i(t)\right)^T \tag{38}$$

$$\frac{\partial \mathbf{h}_{Pos}}{\partial \mathbf{b}_{se}}(\hat{\mathbf{x}}) = \mathbf{I}_{3\times 3} \tag{39}$$

Notice that this is a linear measurement and the measurement noise is given by the displacement due to sway.

IV.C. Zero Velocity

The zero velocity measurement is expressed as follows:

$$\mathbf{y}_{ZV} = \mathbf{h}_{ZV}(\mathbf{x}, t) = \left(\mathbf{T}_e^i(t)\right)^T \left(\mathbf{v}^i - \boldsymbol{\omega}_E^i \times \mathbf{r}^i\right) + \boldsymbol{\eta}_{ZV} = \mathbf{0} \tag{40}$$

where $\boldsymbol{\omega}_E^i$ is the Earth angular velocity vector and $\boldsymbol{\eta}_{ZV}$ is the measurement noise which exactly cancels out the motion due to twist and sway. The estimated measurement is given by

$$\hat{\mathbf{y}}_{ZV} = \mathbf{h}_{ZV}(\hat{\mathbf{x}}, t) = \left(\mathbf{T}_e^i(t)\right)^T \left(\hat{\mathbf{v}}^i - \boldsymbol{\omega}_E^i \times \hat{\mathbf{r}}^i\right) \tag{41}$$

The measurement residual is

$$\boldsymbol{\epsilon}_{ZV} = \mathbf{y}_{ZV} - \hat{\mathbf{y}}_{ZV} = \mathbf{H}_{ZV}(\hat{\mathbf{x}})\,\hat{\mathbf{x}} + \boldsymbol{\eta}_{ZV} \tag{42}$$

With this in mind, the partial derivative of the zero velocity measurement is as follows

$$\frac{\partial \mathbf{h}_{ZV}}{\partial \mathbf{r}}(\hat{\mathbf{x}}) = \left(\mathbf{T}_e^i(t)\right)^T \left[\boldsymbol{\omega}_E^i \times\right] \tag{43}$$

$$\frac{\partial \mathbf{h}_{ZV}}{\partial \mathbf{b}_{se}}(\hat{\mathbf{x}}) = \left(\mathbf{T}_e^i(t)\right)^T \tag{44}$$

Notice that this is a linear measurement and the measurement noise is given by the velocity of the oscillation due to sway.

IV.D. Fine Align Measurement Trade

During factor of safety performed prior to EFT-1, the analysis showed that the IV measurement is subject to divergence under some higher-than-expected frequency cases. These cases were deemed extremely unlikely and since the performance was monitored from the ground which could scrub the launch if the atmospheric conditions created excessive motion of the stack. While robustness to the amplitude of the oscillations can be achieved via tuning of the value of the IV measurement noise variance, increasing robustness to very large frequency variations presents a less obvious solution. The issue is that high frequency of oscillation make the IV measurement nonlinearities more pronounced.

The IV measurement is inherently a measurement of velocity, or at least average velocity, since it measures the change in position. Therefore this measurement type provides very little information on the position of the vehicle, which can be seen by the gradual increase of the position estimation error covariance returned by the filter during fine align. Very long ground operations can cause the position estimation error to become excessively large, forcing the ground to send a position re-anchoring command prior to launch, as routinely done in the Space Shuttle. Two options are possible, overwriting the state only, hence having a good state estimate but a large, over conservative estimation error covariance. Or to re-initialize the position error covariance as well, hence loosing the correlations with all the remaining states built during fine align.

In fact, during very long pad alignment times, the position covariance eventually ceases to increase and asymptotically settles to a large value. The reason is that some information is extracted from the gravity model and the measurement of gravity. Since the position of the pad is known with a certain uncertainty, a desirable design is one in which the position estimate and its uncertainty are constant (in Earth-fixed coordinates) while all other states are estimated. This can be achieved by the pad position measurement.

These two facts have lead to a trade study of possible solutions to alleviate the issues and create a better design.

The most important aspect of the trade is whether or not a position re-anchoring is necessary. Ground commands not only increase the complexity of the code, but, more importantly, require controllers to spend considerable time developing and studying flight rules to handle various scenarios. A position re-anchoring can be automatically forced immediately prior to launch, however this has the unwanted side effect of either a largely conservative position covariance, or cancelling all the correlation between position and other states, which in turn are used to estimate the other states from pseudo range measurements during ascent. The pad position measurement keeps the estimated position error covariance constant during ground align operations, and never necessitates of a re-anchoring. Both IV and ZV measurement have very weak position observability, which comes from either the fact that gravity is a function of position or from $\omega \times \mathbf{r}$ due to Earth's rotation; goth have a very low sensitivity to position changes.

In all aspects of flight software design, it is also very important to keep the algorithm as simple as possible while meeting requirements. ZV and Pos measurements are both linear, do not require back propagation of the state, and hence are significantly simpler to implement than IV. Of the two, ZV is the simpler because it does not require the addition of any other state. The need of pad position bias states is imperative in processing pad measurement. The survey error is done only once, therefore processing the measurement every second results in a constant error, furthermore this survey value is used to initialize the filter, hence the initial error is correlated to the measurement error. The need for extra states, and hence a larger covariance matrix and more computations, is highly mitigated by the fact that GPSR measurement are not processed while on the pad and they also necessitate extra states. Therefore the GPS clock bias and drift states for the two receivers are recycled as pad position bias states. As a result the pad position measurement does not require any increase on the size of the EKF state vector.

While filter divergence is a very serious issue that must be taken into consideration, the situations in which IV measurement caused divergence of the filter were extreme and deemed very unlikely to occur. Even if they did occur, it would probably be due to bad weather and monitored by the ground which would postpone the launch. Therefore divergence issues are the lowest weighted element of the trade. Pad position and ZV are linear measurements, therefore they cannot cause divergence during a measurement update (divergence can occur during propagation, but that is completely independent from the choice of measurement update).

Given these three aspects of the trade, pad position measurements were deemed the best solution for Orion going forward and replaced IV for Exploration Mission 1 and beyond. Table 1 shows the matrix of the trade.

Table 1. Fine Align Measurements Trade Matrix

Trade Factor	Trade Weight	IV	Pos	ZV
Avoid position re-anchor	High	NO	**YES**	NO
Lower algorithm complexity	Medium	NO	NO	**YES**
Avoid potential divergence	Low	NO	**YES**	NO

IV.E. Exploration Mission I Design

The Orion atmospheric extended Kalman filter (ATMEKF) processes all available observations each cycle to estimate position, velocity, and alignment, along with the measurement error parameters. All inertial sensor error estimates are fed back as corrections each cycle during the INS state correction process. The U-D-U algorithm is used in the ATMEKF processing to avoid any possible numerical instability.

From the trade study discussed above, the pad position measurement is processed by the filter. The observation is based on the fact that, during ground alignment, the navigation base is not moving with respect to Earth, other than twist and sway. The surveyed position of the stack is therefore used as an external measurement and it is compared to the propagated position using gravity and IMU data. This observation can be mapped directly into the integrated position state via the Earth-Fixed to Inertial transformation matrix. Two errors affect the measurement. The first is due to oscillations because of twist and sway, this error source is aleatory in nature and modeled as white noise. The second source of error is repeatable, and is given by the survey error of the pad location together with the error in establishing the position of the IMUs with respect to the pad. This error is accounted for as a state in the filter.

The normalized squared measurement residuals values for each of the three components of the position

observation are calculated prior to processing any observations. If any of the three values values exceeds the limit, all observation components are discarded for this cycle.

The state vector components are divided in dynamic-states and parameter-states. Parameter-states differ from the other states in that they are modeled as first order Markov processes, therefore their time evolution is known analytically and does not necessitate numerical integration. In addition, their state transition matrix is also known analytically and it is very sparse, making their covariance matrix propagation extremely numerically efficient.

The states are partitioned into vehicle dynamic states, $\mathcal{X}$, and the parameter-states (IMU errors, GPS PR errors), $\mathcal{B}$, so that

$$\mathbf{X} = \begin{bmatrix} \mathcal{X}^T & \mathcal{B}^T \end{bmatrix}^T \tag{45}$$

We explicitly include the attitude as a state in order to properly model the coupling inherent in a strap-down IMU (particularly during accelerated flight). As stated earlier the parameter-states are modeled as first-order Gauss-Markov processes and use a much more efficient computational algorithm for the update of the covariance matrix. Tables 2 and 3 list the states and parameters within the Atmospheric EKF.

Table 2. Atmospheric Navigation States

State	Number of elements	Description
Position	3	Position vector in inertial coordinates
Velocity	3	Velocity vector in inertial coordinate
Attitude	3	Multiplicative attitude deviation state
Clock Bias and Drift	4	One pair per receiver, three of these states are used as pad position bias states during fine align

Table 3. Atmospheric Navigation Parameters

Parameter	Number of elements
gyro bias	3
gyro scale factor	3
accel bias	3
accel scale factor	3
pseudorange bias	12

Position, velocity, and attitude states and their covariance are initialized as appropriate directly from data provided to the CSU. During Pad initialization scenarios, states 10 to 12 are initialized as pad bias states. The pad position measurement is expressed in the ITRF and is modeled as

$$\mathbf{y}_{pad} = \mathbf{r}^e + \mathbf{b}^e_{pad} + \boldsymbol{\eta}_{pad}$$

where $\mathbf{r}^e$ is the ITRF position vector, $\mathbf{b}^e_{pad}$ is the survey error of the pad position, and $\boldsymbol{\eta}_{pad}$ is the non-repeatable error of the measurement (e.g. due to twist and sway motion). The filter is initialized with the pad surveyed position coordinated in the inertial frame, that is, the initial position estimate is given by

$$\hat{\mathbf{r}}(t_0) = \mathbf{T}^i_e(t_0)\,\mathbf{y}_{pad}$$

where $\mathbf{T}^i_e$ is the DCM transforming inertial coordinates into ICRF coordinates, therefore the initial position estimation error $\mathbf{e}_r(t_0)$ is given by

$$\mathbf{e}_r(t_0) = \mathbf{r}(t_0) - \hat{\mathbf{r}}(t_0) = \mathbf{T}^i_e(t_0)\mathbf{r}^e - \mathbf{T}^i_e(t_0)(\mathbf{r}^e + \mathbf{b}^e_{pad} + \boldsymbol{\eta}_{pad}) \tag{46}$$

$$= -\mathbf{T}^i_e(t_0)\mathbf{b}^e_{pad} - \mathbf{T}^i_e(t_0)\boldsymbol{\eta}_{pad} = -\mathbf{T}^i_e(t_0)\mathbf{e}^e_{b_{pad}} - \mathbf{T}^i_e(t_0)\boldsymbol{\eta}_{pad} \tag{47}$$

The last equality holds because the initial estimated pad survey error is zero (otherwise the estimate error would be subtracted from the estimated position resulting in a new estimated position with zero estimated error). Equation (47) shows the correlation between the initial position and the survey error state, from it we deduce the values for the following elements of the initial covariance matrix

$$\mathbf{P}_0(b_{pad}, b_{pad}) = \mathbf{T}_i^e(t_0)\ \mathbf{P}_0(r,r)\ \mathbf{T}_e^i(t_0) \tag{48}$$

$$\mathbf{P}_0(X, b_{pad}) = \mathbf{P}_0(X,r)\ \mathbf{T}_e^i(t_0) \tag{49}$$

$$\mathbf{P}_0(b_{pad}, X) = \mathbf{T}_i^e(t_0)\ \mathbf{P}_0(r,X) \tag{50}$$

where $\mathbf{P}_0(b_{pad}, b_{pad})$ is the 3×3 covariance of the pad survey error state, $\mathbf{P}_0(r,r)$ is the 3×3 initial covariance of the position state, $\mathbf{P}_0(X, b_{pad})$ is the cross covariance between any state X and the pad survey error state. The resulting 12x12 position, velocity, attitude, and pad survey error covariance matrix is generally non-diagonal and is converted to its UDU factorization for the filter to use. During non-pad initialization cases, states 10 to 12 are left unitialized; they will be initialized, together with state 13, once valid GPS measurements are received by the filter.

V. Pre-Launch EFT-1 Performance

Process noise is used to tune the filter. For the Orion Absolute Navigation Filter, the process noise enters the covariance update via the dynamic states and the parameter states. For the position and velocity, the process noise enters via the velocity state; the process noise represents the uncertainty in the dynamics, chiefly caused by mis-modeled (or unmodeled) accelerations. Since the accelerometers only measure non-inertial forces, gravity is modeled via a high-order gravity model. For the Orion Absolute Navigation filter, Earth's gravity is modeled by an 8×8 gravity field; higher-order spherical harmonics are neglected and hence are captured by the velocity process noise. Additionally, since the attitude rate states are not part of the filter, the attitude process noise enters via the gyro angle random walk. The velocity and attitude process noises are obtained from the IMU Velocity Random Walk and Angular Random Walk performance, respectively. Conservative values of 0.96741 ft^2/s and 0.0096741ft^2/s^3 are used for the clock bias and drift process noise, respectively.

The IMU states are modeled as first-order Gauss-Markov processes and carry with them corresponding process noise parameters which are used in the tuning of the filter. Since the IMU errors were expected to be quite constant during the 4.5 hour flight, the time constant of these parameters was chosen as 4 hours, and the process noise was chosen such that the steady-state value of the Markov processes was equal to the vendor's specification.

During fine align the navigation filter process integrated velocity (IV) measurements. Figure 1 shows the performance of the filter processing this measurement by means of the measurement residual (actual measurement minus estimated measurement, blue lines) and their predicted covariance (red lines). It can be seen that the residuals are well within their predicted variance, all of the measurements are accepted (green line) and zero rejections occur (red line). The residuals are extremely small with respect to their predicted standard deviation, this suggests the filter is overly conservative. This fact was expected and a design choice to add robustness to large twist and sway motion of the launch vehicle. During the day of flight little to no twist and sway was observed. Figure 1 shows the results from Channel 1. A zoomed in plot of the residuals from Channel 2 is shown in Figure 2. Throughout the flight the performance of the two channels is nearly identical, therefore only results from Channel 1 are shown for the remainder of this paper.

Figure 3 shows the filter's position, velocity, and attitude covariance. Figures 4 and 5 show the accelerometer and gyro error states covariance, respectively. Figures 6 and 7 show the filter's estimates of the accelerometer and gyro errors, respectively. The performance is as expected.

Finally, Figures 8 to 10 show the position, velocity, and attitude estimates from the user parameters processor (UPP) which provided the outputs from channel 1.

VI. Conclusions

This paper documents the design of the Orion ground navigation system and presents its performance during Exploration Flight Test 1 (EFT-1). Characteristics of the EFT-1 design were introduced, and data from the flight is shown to validate the design choices. This data illustrates a flight in which the absolute

navigation system performed as expected and produced a good state to guidance and control. No Integrated Velocity measurement rejections occurred in the filter and the measurement residuals were very low with respect to their predicted standard deviations. This fact is due to a combination of conservative tuning of this measurement and perfect weather during the day of launch. Design trades are also presented to justify the transition from the EFT-1 IV measurement to the use of Pad Position measurement during future Exploration Mission flights. The design of the EM1 ground alignment phase is presented in detail.

References

[1]R. Zanetti, G. N. Holt, R. S. Gay, C. D'Souza, and J. Sud, "Orion Exploration Flight Test 1 (EFT1) Absolute Navigation Performance," Presented at the 2016 AAS/AIAA Space–Flight Mechanics Meeting, Napa, CA Feb 14–18 2016. AAS 16-201.

[2]A. Gelb, ed., *Applied Optimal Estimation*. Cambridge, MA: The MIT press, 1974.

[3]J. Sud, R. Gay, G. Holt, and R. Zanetti, "Orion Exploration Flight Test 1 (EFT1) Absolute Navigation Design," *Proceedings of the AAS Guidance and Control Conference*, Vol. 151 of *Advances in the Astronautical Sciences*, Breckenridge, CO, January 31–February 5, 2014 2014, pp. 499–509. AAS 14-092.

[4]G. Holt, R. Zanetti, and C. D'Souza, "Tuning and Robustness Analysis for the Orion Absolute Navigation System," Presented at the 2013 Guidance, Navigation, and Control Conference, Boston, Massachusetts, August 19–22 2013. AIAA-2013-4876, doi: 10.2514/6.2013-4876.

[5]G. J. Bierman, *Factorization Methods for Discrete Sequential Estimation*, Vol. 128 of *Mathematics in Sciences and Engineering*. Academic Press, 1978.

[6]N. A. Carlson, "Fast Triangular Factorization of the Square Root Filter," *AIAA Journal*, Vol. 11, September 1973, pp. 1259–1265.

[7]W. Agee and R. Turner, "Triangular Decomposition of a Positive Definite Matrix Plus a Symmetric Dyad with Application to Kalman Filtering," Tech. Rep. 38, White Sands Missile Range, White Sands, NM, 1972.

[8]S. F. Schmidt, "Application of State-Space Methods to Navigation Problems," *Advances in Control Systems*, Vol. 3, 1966, pp. 293–340.

[9]R. Zanetti and C. D'Souza, "Recursive Implementations of the Consider Filter," *Journal of the Astronautical Sciences*, Vol. 60, July–December 2013, pp. 672–685. doi: 10.1007/s40295-015-0068-7.

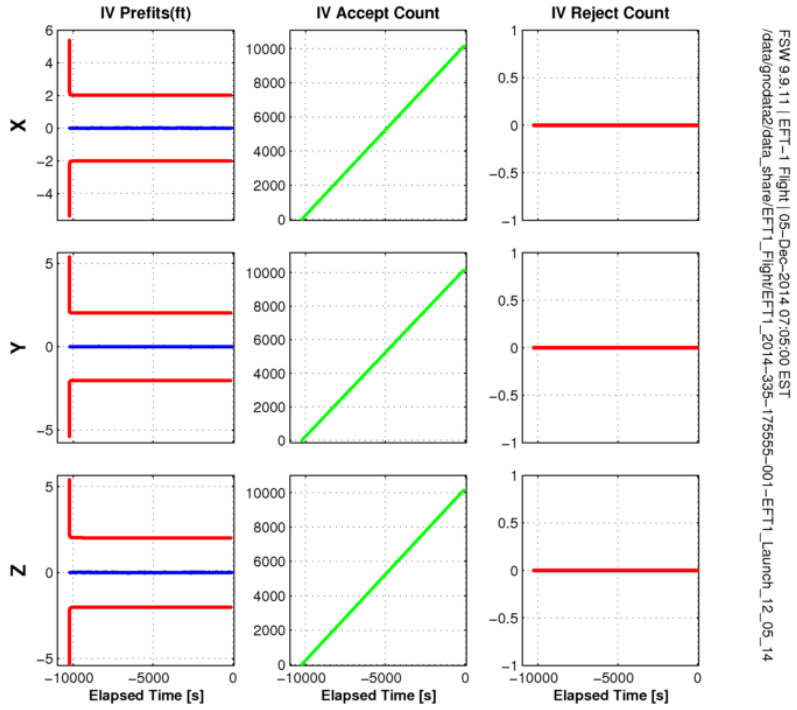

Figure 1. FCM1-CH1 IV Measurements

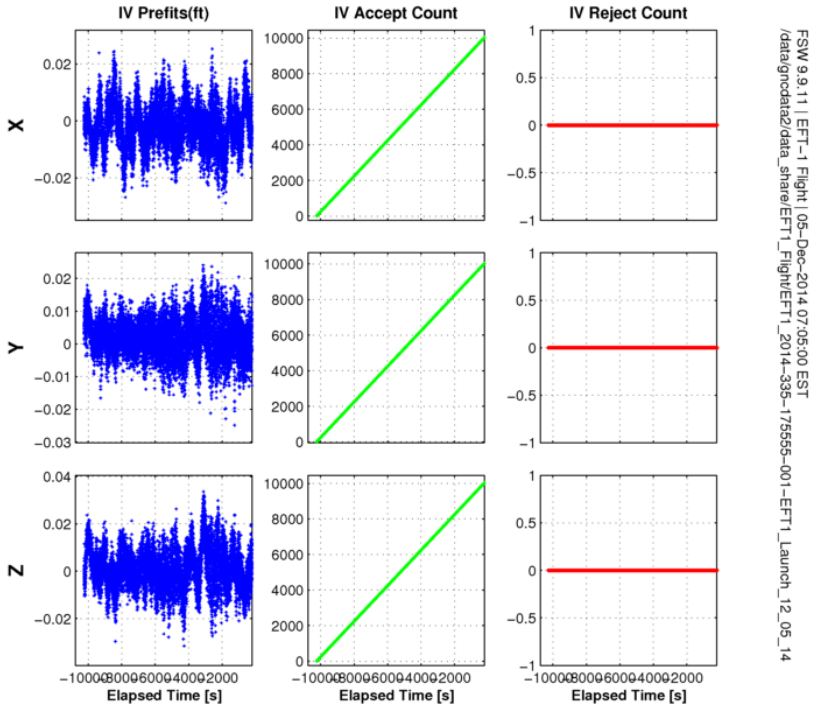

Figure 2. FCM1-CH2 IV Measurements

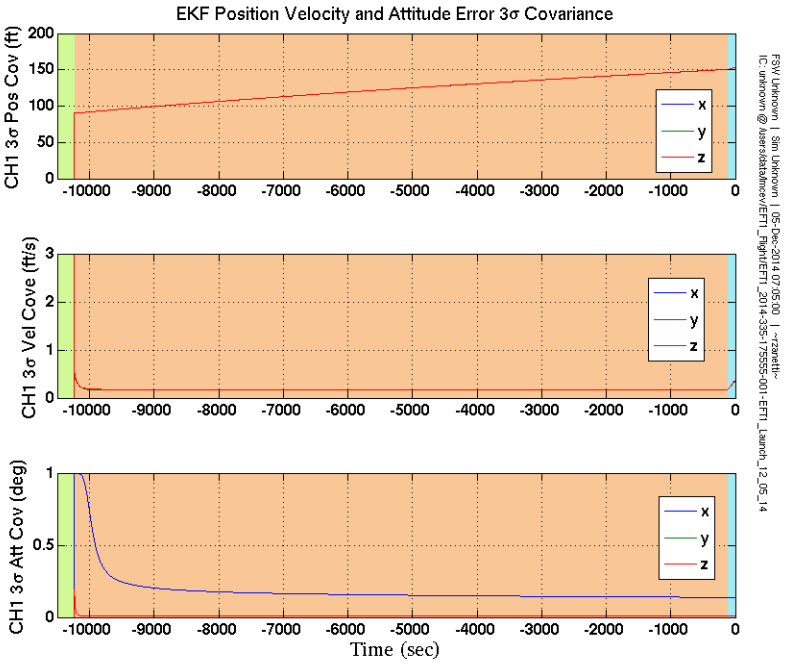

Figure 3. FCM1-CH1 Position, Velocity, and Attitude 3σ Covariance

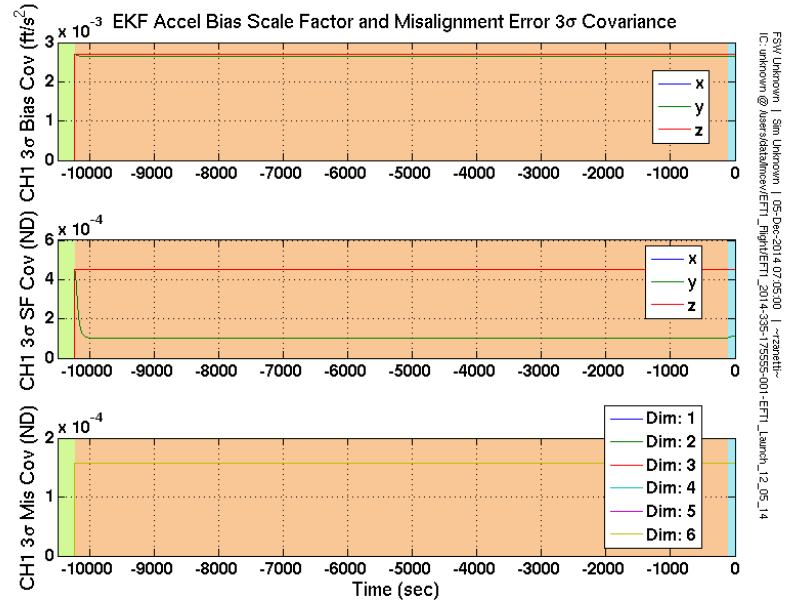

Figure 4. FCM1-CH1 Accelerometer Bias, Scale Factor, and Misalignment 3σ Covariance

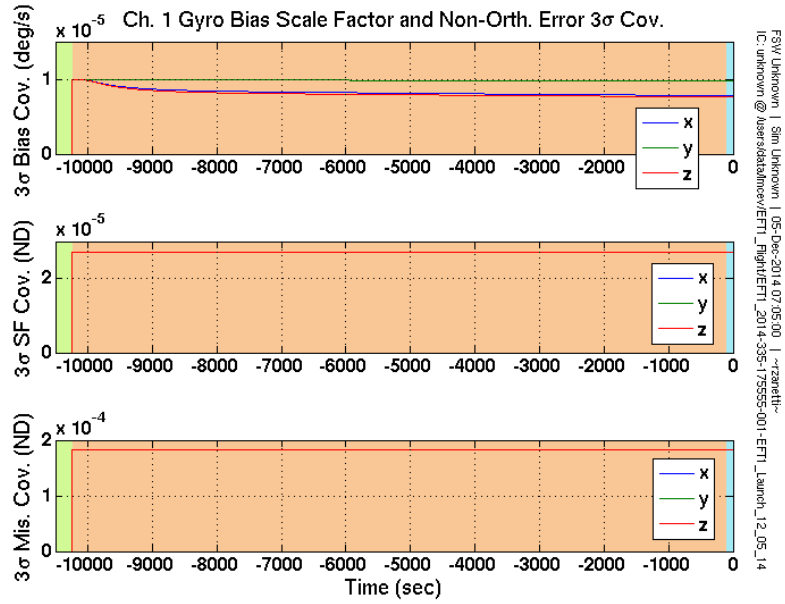

Figure 5. FCM1-CH1 Gyro Bias, Scale Factor, and Non-Orthogonality 3σ Covariance

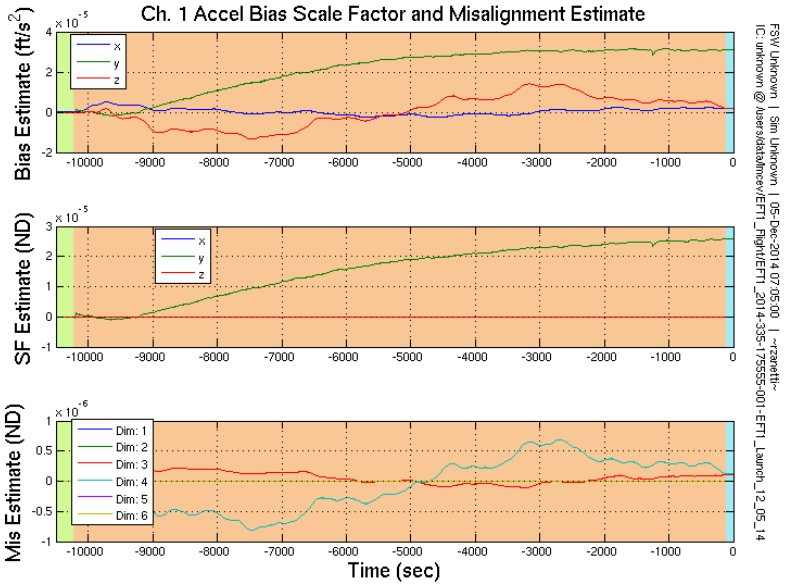

Figure 6. FCM1-CH1 Accelerometer Bias, Scale Factor, and Misalignment Estimate

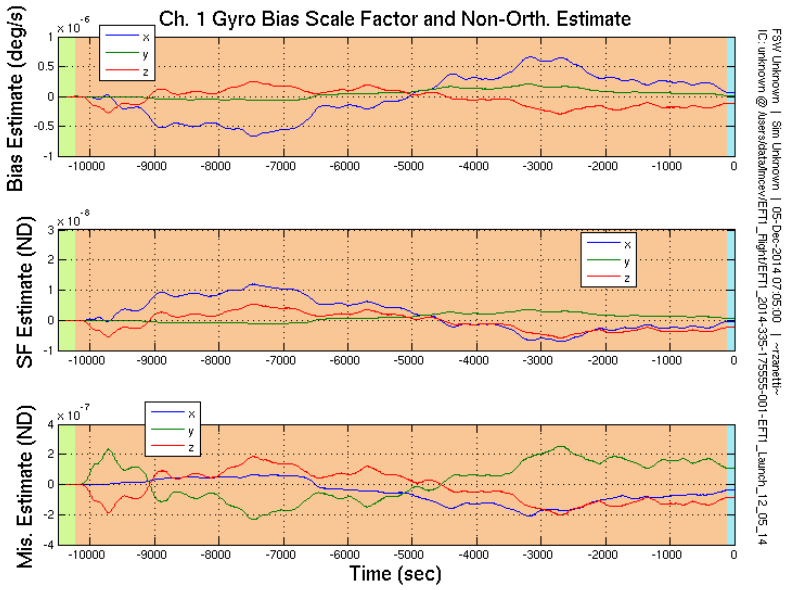

Figure 7. FCM1-CH1 Gyro Bias, Scale Factor, and Non-Orthogonality Estimate

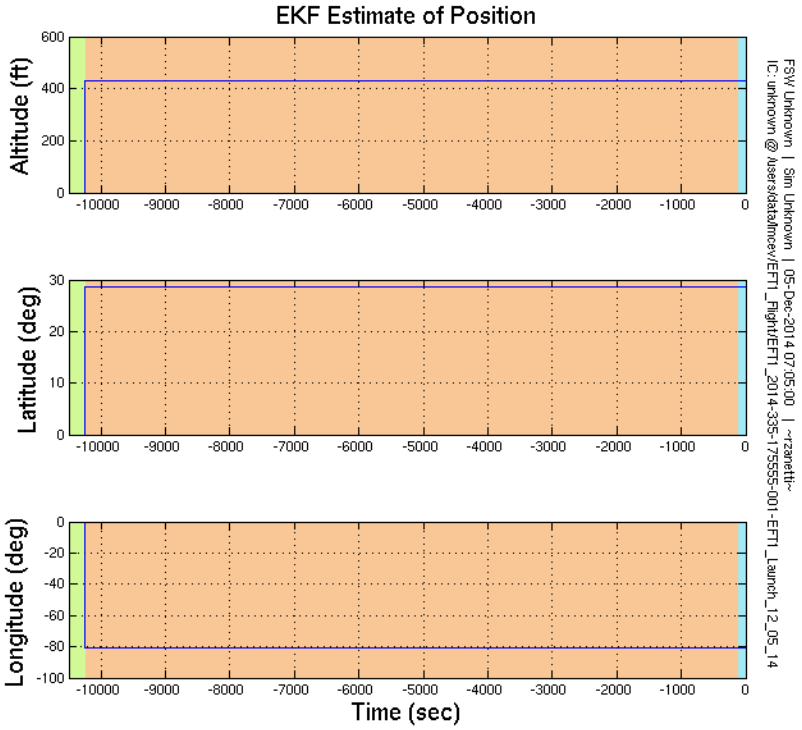

Figure 8. FCM1-CH1 Position Estimate

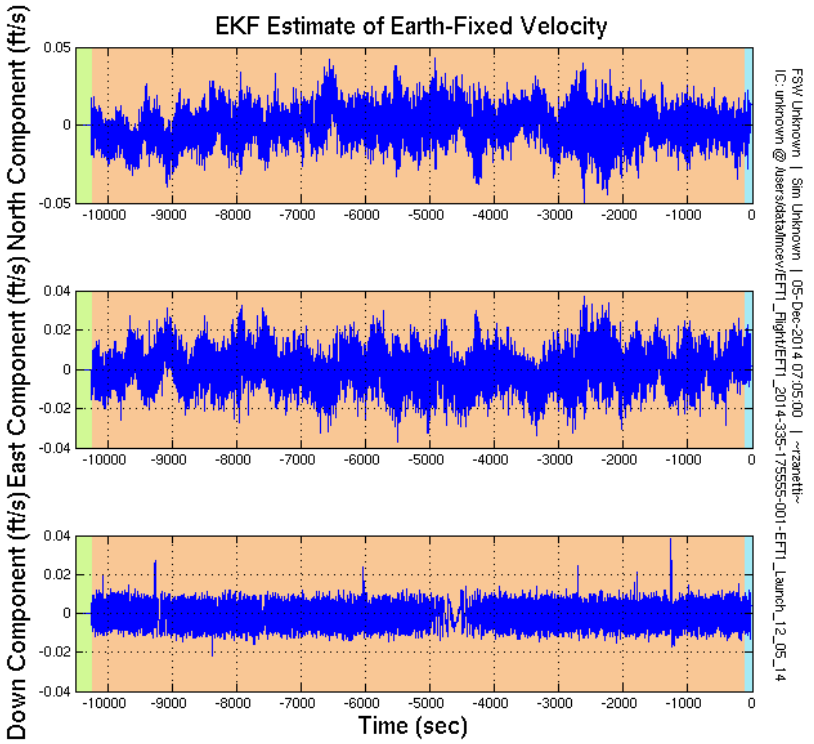

Figure 9. FCM1-CH1 Velocity Estimate

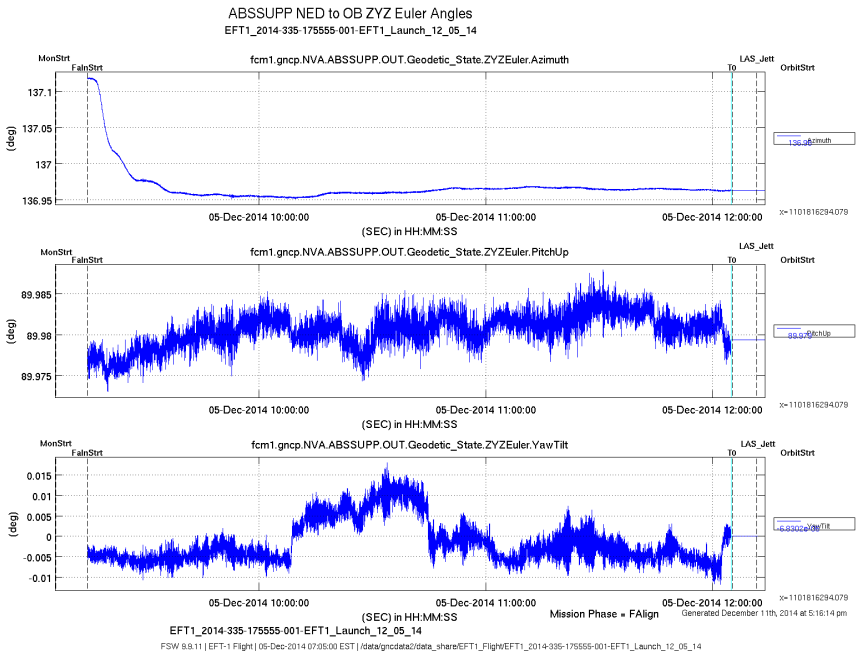

Figure 10. FCM1-CH1 Attitude Estimate